Volume 7
Number 5
May 2020
Pages 1277–1620

Environmental Science Nano

rsc.li/es-nano

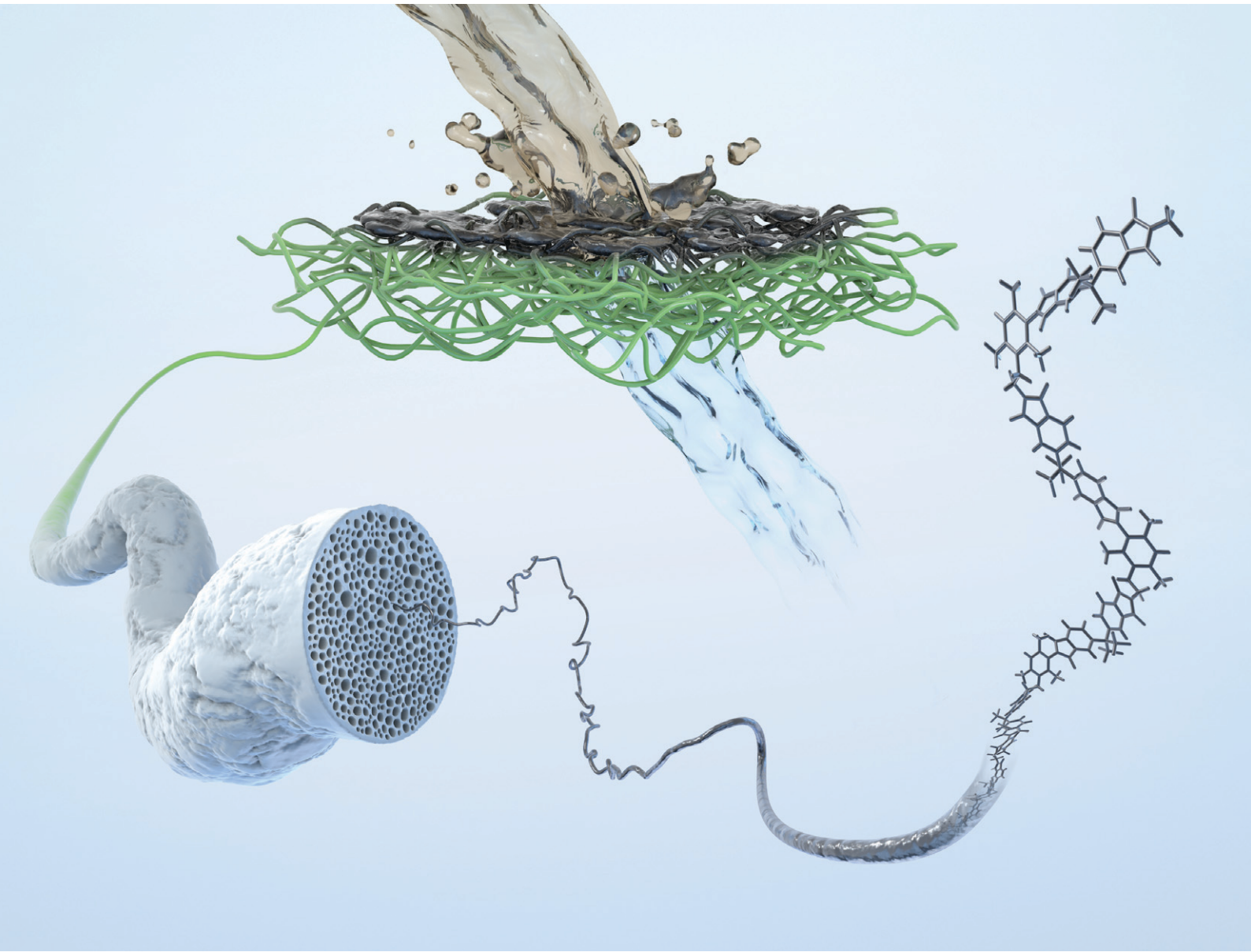

ISSN 2051-8153

ROYAL SOCIETY OF CHEMISTRY

PAPER

Fuat Topuz, Gyorgy Szekely *et al.*

Hierarchically porous electrospun nanofibrous mats produced from intrinsically microporous fluorinated polyimide for the removal of oils and non-polar solvents

Environmental Science Nano

ROYAL SOCIETY OF CHEMISTRY

PAPER

View Article Online
View Journal | View Issue

Cite this: *Environ. Sci.: Nano*, 2020, 7, 1365

Hierarchically porous electrospun nanofibrous mats produced from intrinsically microporous fluorinated polyimide for the removal of oils and non-polar solvents†

Fuat Topuz, *[a] Mahmoud A. Abdulhamid, [a] Suzana P. Nunes [ab] and Gyorgy Szekely *[ac]

Received 20th January 2020,
Accepted 17th March 2020

DOI: 10.1039/d0en00084a

rsc.li/es-nano

Oil spills impose serious ecological threats to the environment and are of international concern. Novel approaches and materials are continuously being sought to improve the cleanup of oil spills. In widespread oil spills, the performance of many materials used as oil sorbents is limited by their low surface area. Here, we describe a novel nanofibrous oil sorbent composed of a fluorinated polyimide of intrinsic microporosity (PIM-PI) with a high Brunauer–Emmett–Teller (BET) surface area of 565 $m^2 g^{-1}$. The nanofibrous sorbent was produced by electrospinning of PIM-PI (6FDA–TrMPD), which was synthesized by a one-pot, high-temperature polycondensation reaction between 4,4′-(hexafluoroisopropylidene)diphthalic anhydride (6FDA) and 2,4,6-trimethyl-*m*-phenylenediamine (TrMPD). Electrospinning of 6FDA–TrMPD from a solution of DMF with a concentration of 10% (w/v) produced ultrafine nanofibers, whereas at lower concentrations, beaded-fibers were obtained. The adsorption performance of the nanofibrous sorbent using several oils (*i.e.* crude oil, silicone oil, gasoline, and diesel) and non-polar organic solvents (*i.e.* toluene and *m*-xylene) was explored. The developed sorbent showed high sorption capacities in the range of 25–56 g g^{-1}, along with a rapid removal performance; the sorbent reached the equilibrium sorption capacity within a few minutes for oils and organic solvents. The feasibility of the designed hierarchically porous mat for oil spill cleanup was demonstrated by the treatment of real seawater and crude oil. The robustness and reusability of the sorbent were demonstrated through its regeneration by both mechanical recovery and toluene treatment.

Environmental significance

Oil spills can cause significant damage to the marine ecosystem and human life. This has sparked a great demand for high-efficiency, innovative sorbents that can thoroughly clean up water resources. Here, we present a novel nanofibrous sorbent material with a hierarchically porous structure as an excellent option. In brief, the structure is derived from an intrinsically microporous fluorinated polyimide, with the electrospinning of the polymer boosting the surface area of the nanofiber from 450 to 565 $m^2 g^{-1}$, mainly by inducing mesopores. During the electrospinning process, macropores are formed between the intertwined fibers, creating both micro- and macropores that allow the rapid removal of oils and non-polar solvents. We successfully used the new sorbents for removing crude oil from seawater, and subsequently regenerated them mechanically or by toluene treatment. This opens new avenues for developing high-performance sorbent systems, not only for oil removal but also for scavenging of water micropollutants.

1. Introduction

Frequent and devastating oil spills have caused widespread ecological disasters over the past century. Tremendous effort has been made to develop sorbents that are capable of removing these oil spills from the environment more rapidly and efficiently.[1,2] Oil spills that occur in aqueous environments are subjected to various processes, such as spreading, evaporation, drifting, partial dissolution, photolysis, biodegradation, and the formation of water/oil emulsions.[3,4] These processes make cleanups of oil spills at sea especially complicated, with

[a] *Advanced Membranes and Porous Materials Center, Physical Science and Engineering Division (PSE), King Abdullah University of Science and Technology (KAUST), Thuwal, 23955-6900, Saudi Arabia. E-mail: fuat.topuz@kaust.edu.sa, gyorgy.szekely@kaust.edu.sa; Tel: +966128082769*
[b] *Biological and Environmental Science and Engineering, King Abdullah University of Science and Technology (KAUST), Thuwal, 23955-6900, Saudi Arabia*
[c] *Department of Chemical Engineering and Analytical Science, University of Manchester, The Mill, Sackville Street, Manchester M1 3BB, UK. E-mail: gyorgy.szekely@manchester.ac.uk*

† Electronic supplementary information (ESI) available: Polymer and material characterization, and video of emulsion separation. See DOI: 10.1039/d0en00084a

significant detrimental impacts on marine ecosystems, human health, and the greater environment. Because of their lipophilic nature, oil residues can accumulate in organic matter and sediments, and can form oil/water emulsions.[5] Moreover, the contamination of rivers with organic solvents reduces access to clean water resources for dependent populations, and endangers the ecosystems of the rivers.[6] Thus, a rapid response to and prompt cleanup of oil spills from water resources is crucial.

Various foams and sponges have been developed to mitigate and clean up spills that have occurred in the aquatic environment.[7–11] Sponges and foams have large macropores and structural stability that make them ideal sorbents for oil cleanup. For example, highly durable superhydrophobic foams have been fabricated by combining extrusion and supercritical CO_2 foams for selective oil sorption.[12] These superhydrophobic foams show an adsorption capacity range between 4.6 and 9.1 g g^{-1} and high stability, even following repetitive reuse after mechanical recovery. Another sponge for oil cleanup has been developed using carbon soot through a dip-coating method,[13] showing high absorption capacities (25–80 g g^{-1}) for a broad spectrum of oils and organic solvents. In particular, the sorption capacity of the sorbent for crude oil was found to be 30 g g^{-1}. Likewise, Fe/C nanocomposites (4.5–7.5 g g^{-1}),[14] nanocellulose aerogels (20–40 g g^{-1}),[15] porous poly(dimethylsiloxane) (4–34 g g^{-1}),[16] and graphene sponge (20–86 g g^{-1})[17] have also been proposed for oil cleanup. As an alternative to these materials, electrospun mats have attracted increasing interest because of their tunable structural properties. Recyclable porous polyacrylamide/polystyrene fibers are produced by electrospinning and have been previously employed for oil/water separation.[18] Nanofibrous superhydrophobic membranes embedded with Au nanoparticles have been successfully employed for both oil/water separation and catalytic degradation of 4-nitrophenol.[19] Likewise, a mixed matrix electrospun mat comprising of polyacrylonitrile and Au@ZIF-8 nanoparticles (with the subsequent surface decoration of the nanofibers using tannic acid and 1-dodecanethiol) has been developed for oil/water de-emulsification. Shami *et al.* described a superoleophobic nonwoven mesh for oil/water separation using a modified styrene–acrylonitrile copolymer,[20] where the electrospun fibers were treated with a hot aqueous solution of NaOH to produce pH-responsive carboxylic acid groups, and the fibers were successfully used for immiscible/emulsified light oil–water separation. A flexible, durable magnetic nanofibrous membrane with pH-switchable wettability for on-demand oil/water separation was developed.[21] Superoleophobic nanofibrous membranes from poly(vinyl alcohol) and graphene oxide were also proposed for emulsified oily water purification.[22] Nature-inspired solutions were also developed, for instance radially distributed nanofibrous membranes for continuous oil–water separation.[23]

PIM-based electrospun materials were also used for oil–water removal and oil/water separation. Electrospun microfibrous membranes of PIM-1 containing 40 wt% POSS,[24] and a blend of hydrolyzed PIM-1 and hexamethylene diisocyanate was electrospun and thermally cured at 150 °C,[25] were fabricated and used for separation of oil/water mixtures and cleanup of oil soluble contaminants. The fiber mat was employed for the removal of several oils and organic solvents, as well as oil/water separation. A comprehensive review of the use of electrospun materials for oil removal has been recently compiled.[26]

In this study, we design a hierarchically porous nanofibrous mat for the removal of oil and non-polar solvents (Fig. 1). We describe an intrinsically microporous polyimide with pendant trifluoromethyl ($-CF_3$) motifs that is electrospun into mesoporous nanofibers, thus forming a mat with macropores. To the best of our knowledge, the use of electrospun sorbents produced from intrinsically porous polyimides has not yet been reported in the literature.

2. Experimental

2.1 Materials

4,4′-(Hexafluoroisopropylidene)diphthalic anhydride (6FDA, 99%), 2,4,6-trimethyl-*m*-phenylenediamine (TrMPD, 96%), *m*-cresol (99%), and isoquinoline (97%) were obtained from Merck and used as received without further purification. Dimethylformamide (DMF, 99.9%) was purchased from Fischer. Toluene (99.9%, Burdick & Johnson), *m*-xylene (98.6%, VWR Normalur Analar), and hexane (HPLC grade, 99.9%, Sigma) were purchased from Sigma Aldrich. Crude oil (Arabian Light from Saudi Aramco) and silicone oil (for oil baths, Sigma Aldrich) were used as received. Gasoline and diesel were purchased from a local fuel station, while the seawater was collected from the Red Sea (Thuwal, Saudi Arabia).

2.2 Synthesis of the fluorinated porous polyimide

The fluorinated porous polyimide polymer was synthesized by reacting 6FDA (0.59 g, 1.33 mmol) with TrMPD (0.2 g, 1.33 mmol) in *m*-cresol (3 mL) in a 25 mL Schlenk tube equipped with a mechanical stirrer, a nitrogen inlet and an oil bubbler (Scheme 1).[27] The solution was heated to 80 °C and isoquinoline (0.1 mL) was added under nitrogen, followed by stirring at 200 °C for 4 h. Dry nitrogen stream was used to remove water, which resulted from the conversion of polyamic acid to polyimide. The viscous solution was cooled and poured into methanol, resulting in the precipitation of the polymer in a fibrous form, which was collected by filtration and purified twice by re-precipitation from solutions of *N*,*N*-dimethylformamide (DMF) into methanol. Finally, the pale yellowish fibrous material was dried under vacuum for 24 h at 150 °C. The reaction yield was 92%. ^{1}H NMR (400 MHz, DMSO-d_6): δ 1.91 (s, 3H), 2.13 (s, 6H), 7.32 (s, 1H), 7.92 (s, 4H), 8.17 (s, 2H). M_n = 110 987 g mol^{-1}; PDI = 1.59; S_{BET} = 450 ± 15 m^2 g^{-1}; TGA analysis: $T_{d,5\%}$ = 509 °C. FT-IR (ν, cm^{-1}): 2844–2922 (C–H str), 1792 (C═O asym, str), 1724 (C═O sym, str), 1354 (C–N, str). The characteristics of the 6FDA–TrMPD polyimide are provided in Table S1.† The ^{1}H

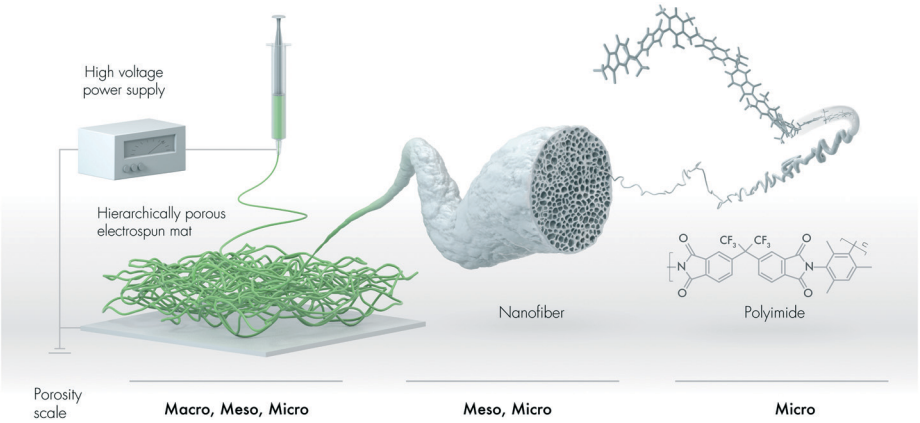

Fig. 1 Schematic illustration of the hierarchically porous nanofibrous mat concept employing an intrinsically microporous polyimide, which is electrospun into nanofibers having meso- and micropores, which are aligned as a 2D mat featuring macro-, meso-, and micropores.

NMR and IR spectra as well as the TGA thermogram of the polymer are shown in Fig. S1–S3.†

2.3 Production of nanofibrous sorbents by electrospinning

The polyimide of intrinsic microporosity (6FDA–TrMPD) at various concentrations was dissolved in DMF under continuous stirring for at least 3 h. The solution was then transferred into a 1 mL disposable plastic syringe (Normjet™ Thermo Scientific) equipped with a sharp-edged metallic needle (Tyco, Kendall 30G). The syringe was placed on a syringe pump (KD Scientific – Legato®) and discharged at a certain speed. A high power voltage supply (SRS, Stanford Research System) was used as the voltage supplier. The nanofibers were collected on a metal collector covered with aluminum foil. During the electrospinning process, the temperature was maintained at 21 °C, and relative humidity was in the range of 50–55%.

2.4 Characterizations

Proton nuclear magnetic resonance (NMR) spectrum of the polymer was recorded with a Bruker AVANCE-III spectrometer at a frequency of 400 MHz using a sample concentration of 15 mg ml^{-1} in DMSO-d_6. The average molecular weight (M_n) and polydispersity index (PDI) of the 6FDA–TrMPD (with a concentration of 1 mg ml^{-1} in DMF solvent) were obtained by gel permeation chromatography (GPC) using an Agilent 1200 system. The molecular weight determined from a calibration curve obtained using polystyrene standards. The decomposition temperatures of the 6FDA–TrMPD before and after electrospinning were acquired with a TGA Q5000 (TA Instruments) at a rate of 5 °C min^{-1} and up to 800 °C. Brunauer–Emmett–Teller (BET) of the 6FDA–TrMPD was measured from a nitrogen adsorption isotherm using a Micrometrics ASAP 2050 porosimetry analyzer. Before the test, all samples were degassed at 150 °C for 16 h at pressures lower than 2 μmHg. The morphology of the electrospun nanofibers was explored by scanning electron microscopy (SEM) (Quanta 600 FEG, FEI and Magellan SEM, FEI). Before SEM analysis, the fiber specimens were coated with 5 nm Pt with a sputtering system. The mean diameter of electrospun nanofibers was determined from the respective SEM images over ~100 nanofibers by ImageJ software (NIH, US National Institutes of Health). XRD analysis was performed on a Bruker D8 ADVANCE in the 2θ range of 3° and 40°. Water contact angle (WCA) and oil contact angle (OCA) measurements were performed on a drop shape analyzer (Krüss Gmph) in triplicate, and the data are reported with standard deviations.

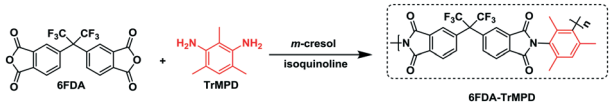

Scheme 1 Synthesis of 6FDA–TrMPD polyimide by a one-pot, high-temperature polycondensation of the 6FDA and TrMPD.

2.5 Oil sorption tests

The electrospun mats were cut in square pieces (10 × 10 mm) and then weighed. The samples were then dipped into 10 mL of crude oil, silicone oil, gasoline, diesel, toluene, and *m*-xylene, and the mass of each mat was measured as a function of time. The experiments were performed in triplicate. The oil sorption capacity (c_{sorp}) was calculated as follows:

$$c_{sorp}\left(\text{g g}^{-1}\right) = \frac{m_t - m_0}{m_0} \quad (1)$$

where m_0 and m_t are the masses of the sample before and after sorption, respectively.

2.6 Nanofiber recovery and reusability

Two different methods were developed for the recovery of the nanofibers. In the first method, following treatment with oil for 5–10 s, the mats were recycled by mechanical recovery and reused 9 times. In the second method, the mat was

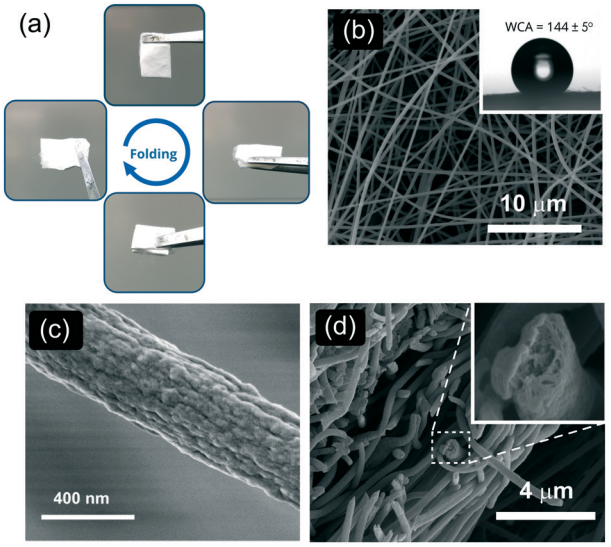

Fig. 2 (a) Optical photos showing the 6FDA–TrMPD mat during the folding/unfolding process, $c_{6FDA-TrMPD}$ = 10% (w/v). (b) SEM image of the nanofibers and its water wettability showing hydrophobicity. (c) SEM image of a single nanofiber showing a wrinkled texture. (d) Cross-section image of the mat and fiber (inset).

rinsed three times with 75 mL toluene for 10 min, and the samples were subsequently dried under vacuum for 3 h at 70 °C. The sorption capacity was calculated using eqn (1). The weights of 6FDA–TrMPD sorbents were recorded before and after each cycle to calculate the sorption capacity.

2.7 Oil/water separation tests

Oil/water separation was carried out using a particular setup, as shown in Fig. S4 and ESI† Video. The sorbent was placed in a vial containing both crude oil and water. The opening of the vial was covered with the fiber mat, and the system was sealed using parafilm at the neck. The vial was kept in a horizontal position, and the crude oil was recovered in a beaker.

3. Results and discussion

The nanofibrous mat was produced by electrospinning the 6FDA–TrMPD from the DMF solutions (Fig. 1). The resulting electrospun mat could be folded without developing any cracks, suggesting it is structurally stable under deformation due to the high molecular weight of 6FDA–TrMPD (Fig. 2a and Table S1†). The dense film prepared from the same polymer also demonstrated high mechanical stability and flexibility (Fig. S5,† Table 1), which allowed the formation of strong nanosheets. Water contact angle (WCA) analysis of the mat revealed its hydrophobic nature, with a respective WCA of 144 ± 5° due to the trifluoromethyl and aromatic groups (Fig. 2b). Oil contact angle (OCA) measurements, using crude oil, silicone oil, gasoline and diesel, show complete wettability of the mat with oil contact angles of less than 1°, demonstrating the superoleophilicity of the mat (Fig. S6†). High-resolution SEM analysis revealed a highly porous texture of the nanofibrous mat (Fig. 2c). The nanofibers themselves have mesopores, which can be attributed to the rapid release of solvent molecules from the nanofiber matrix during the jet formation (Fig. 2d).

The electrospinning of the polyimide was carried out at concentrations ranging from 5% to 12.5% (w/v), and the resulting structures were analyzed by SEM (Fig. 3). The SEM photos of the respective materials show a clear transition from beaded nanofibers to bead-free nanofibers as a result of the increase in polymer concentration. At both 10% and 12.5% (w/v), bead-free nanofibers were formed; however, the mean fiber diameter increased from 187 to 604 nm as a result of higher mass flow. The electrospinning process parameters were further optimized to produce ultrafine nanofibers. First, the applied voltage was gradually increased from 10 to 25 kV, while other parameters, such as tip-to-collector (TCD) and flow rate, were kept constant at 15 cm and 0.5 ml h^{-1}, respectively. Increasing the voltage resulted in the formation of thinner nanofibers (Fig. S7†). The nanofibers electrospun at 10 kV had a mean fiber diameter of 432 nm, which decreased to 298 nm when the applied voltage was increased to 25 kV. Most uniform nanofibers were produced at the applied voltage of 20 kV.

The flow rate was varied to find the optimum value to produce ultrafine fibers. Fig. S8† shows the SEM photos of the nanofibers produced at various flow rates, while the applied voltage and TCD were kept constant at 20 kV and 15 cm, respectively. The increase in the flow rate increased the fiber diameter as a result of a higher mass flow. However, beaded fibers also formed at higher flow rates. The mean diameter of the nanofibers increased from 280 to 380 nm as a result of the 10-fold increase in the flow rate from 0.3 to 3 mL h^{-1}. This phenomenon has been reported previously, where larger and non-uniform fibers were obtained at high flow rates.[28,29] Hence, a lower flow rate is generally recommended to provide the electrospinning solution with enough time for polarization. In contrast, when the solution flow rate is too high, a periodic dripping of the solution will occur. The nanofibers electrospun at the flow rate of 0.6 mL h^{-1} yielded the best uniform fibers among the flow rates tested. We chose the nanofibrous mat produced at the applied voltage of 20 kV and a flow rate of 0.6 mL h^{-1} for a further study on the sorption of oils and non-polar solvents.

Table 1 Mechanical properties of 6FDA–TrMPD film *versus* fibers. Refer to the ESI† for the fabrication of the dense film

Polymer	Tensile strength (MPa)	Tensile modulus (MPa)	Elongation at break (%)
6FDA–TrMPD film	42.6 ± 0.13	1228 ± 37	4.8 ± 0.3
6FDA–TrMPD mat	1.27 ± 0.02	7.12 ± 0.24	27 ± 0.2

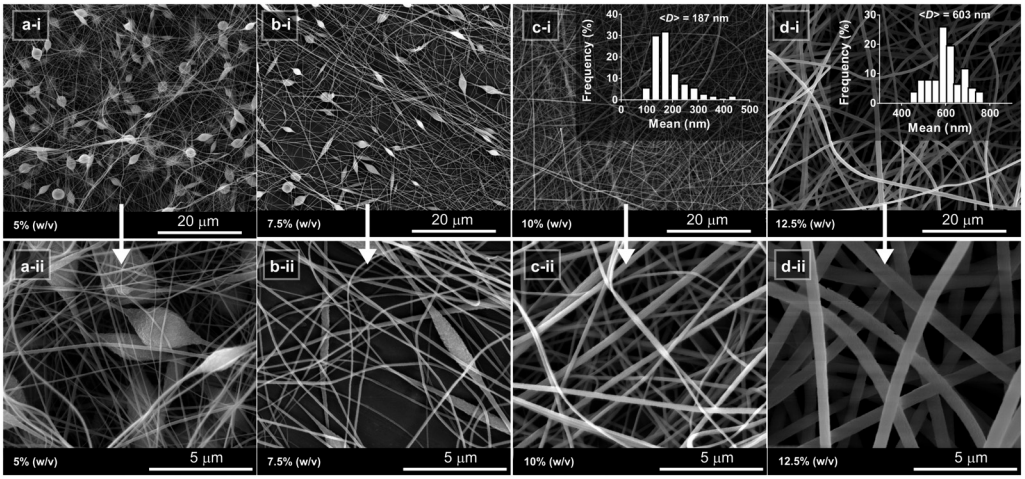

Fig. 3 SEM images showing the influence of polymer concentration on the morphology of the 6FDA–TrMPD nanofibers electrospun from DMF solutions: (a-i and ii) 5%, (b-i and ii) 7.5%, (c-i and ii) 10% and (d-i and ii) 12.5% (w/v). During the electrospinning, the tip-to-collector distance was kept at 15 cm, and the flow rate set to 0.5 mL h^{-1}. Insets (c-i and d-i) show the statistical distribution for the diameter of the respective nanofibers.

Prior to the sorption experiments, the stability of the nanofibers was explored in various solvents after 24 h treatment; SEM images are provided in the ESI† (Fig. S9 and S10). The nanofibers did not show any change in size after incubation in water compared to the pristine sample due to the hydrophobic nature of the polymer (Fig. S9a and b†). However, after treatment with EtOH and hexane, some increase in the fiber diameter was observed (Fig. S9c and d†). The nanofibers exposed to acetonitrile suffered partial decomposition, and the fibrous morphology was lost completely after 24 h incubation (Fig. S9d†). The electrospun mats treated with acetone and ethyl acetate were completely dissolved, while the mats treated with toluene and *m*-xylene maintained the fibrous structure (Fig. S10†).

The electrospinning process did not affect the thermal properties of the 6FDA–TrMPD polymer. The thermal decomposition temperature ($T_{d\ 5\%}$) remained stable at 509 °C (Fig. S3†). However, a 25% increase in the surface area (565 ± 18 $m^2\ g^{-1}$) was observed upon electrospinning of the polymer powder (450 ± 15 $m^2\ g^{-1}$) as shown in Fig. 4a. Moreover, the electrospun 6FDA–TrMPD mat showed a notable enhancement in the pore size distribution in the mesoporous range (2–50 nm, Fig. 4b), confirming the hierarchically porous structure depicted in Fig. 1. Unlike the powder and the electrospun mat, the film counterpart did not exhibit high porosity. The BET surface area for the film was found to be 25 ± 5 $m^2\ g^{-1}$ due to the dense packing of the polymer chains, which inhibits N_2 from penetrating to all pores. The porous structure of the polymer for both powder and nanofiber forms were also explored through WAXS. Fig. 5 shows the XRD patterns of the 6FDA–TrMPD before and after the electrospinning process. Both samples revealed three main peaks at 5.4°, 15.6° and 28.2° with corresponding *d*-spacing values of 17.91 Å, 5.62 Å and 3.08 Å, respectively. These values correspond to the distance between different chain segments and structural polymer groups.[27] The fractional free volume (FFV) of the 6FDA–TrMPD polymer has been previously estimated using Materials Studio and group distribution theory, and it was found to be 25%, which lies in the range that of glassy polymers.[27] We characterized the mechanical properties through stress–strain curves and compared them with the film counterpart; we found the

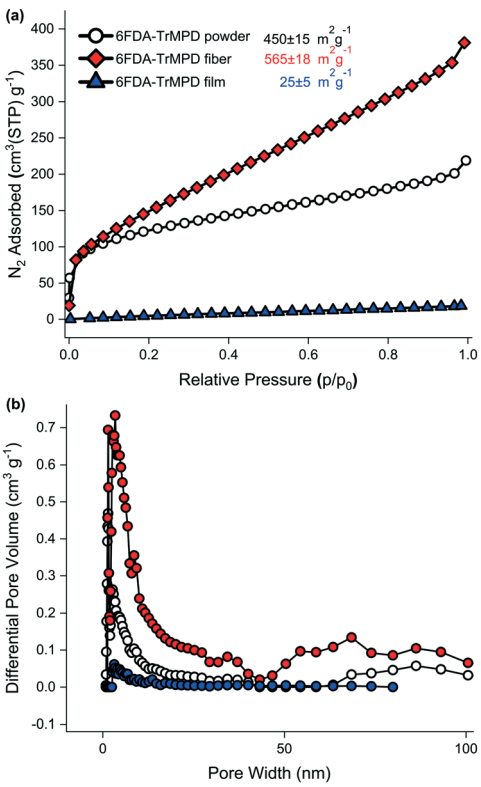

Fig. 4 a) Nitrogen adsorption isotherms measured at −196 °C up to 1 bar, b) NLDFT-derived pore size distributions of the 6FDA–TrMPD polymer powder, the nanofibrous mat and the film.

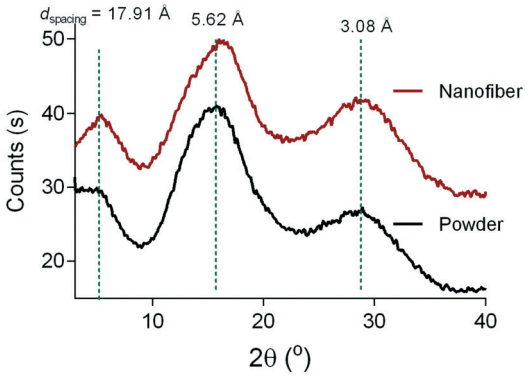

Fig. 5 Wide-angle XRD patterns of the 6FDA–TrMPD polymer and nanofibers.

tensile modulus of the nanofiber mat to be 7.87 MPa, while the nanofibers were ruptured at 27% strain with a corresponding tensile strength of 1.26 MPa (Table 1). A 40 μm-thick film of the same polymer had tensile strength and modulus of 42.6 MPa and 1228 MPa, respectively, while its elongation-at-break was 4.8%. This difference in values (Fig. 4) can be attributed to the fact that the fibers are thinner, and unlike the electrospun nanofibrous mat, the film has a nonporous matrix.

For the oil and non-polar solvent sorption experiments, two different methods were followed (Fig. 6), where the sorbents were either directly exposed to the oils and solvents, or they were exploited to remove oils and solvents from the water surface. The time-dependent sorption kinetics revealed that there was no uptake of water due to the hydrophobic nature of the nanofibers, while the nanofibers exposed to oils and organics showed a drastic mass gain. Interestingly, the nanofibrous mat showed different sorption capacities for gasoline and diesel. Although both are petroleum products, gasoline contains hydrocarbons with, on average, 8 carbon atoms, while diesel possesses, on average, 12 carbon atoms. The 6FDA–TrMPD showed higher affinity for the longer-chain molecules. The sorption kinetics of the materials was rapid, and the sorbents reached their maximum capacities in a few minutes. This rapid sorption capacity can be attributed to the hierarchically porous structure of the electrospun mat, which rapidly adsorbed oils and solvents from the water. The sorption capacities for the spills of oils and organic solvents in the water were lower than their removal from the oils and organics alone, *i.e.* without water.

Moreover, to mimic the removal of oil spills in seas and oceans, the experiments were also performed using seawater (Fig. 6c–e). No significant change in the sorption capacity of the fibers was observed, suggesting that the presence of salt does not affect the sorption performance of the fibers, further demonstrating the practical applicability of the mats for cleaning oil spills. The nanofibrous mat was also exploited for oil/water filtration. A mixture of crude oil and water was filtered through the mat at atmospheric pressure (Fig. S4 and ESI† Video). The crude oil permeated through the membrane, whereas the water was fully retained owing to the hydrophobicity of the mat.

The use of nanofibrous adsorbents is a rapidly growing field of research. Several studies have reported using different polymeric systems and post-modification to enhance the sorption performance of these nanofibrous adsorbents. To the best of our knowledge, the use of electrospun materials (obtained from polyimide of intrinsic porosity (PIM-PI)) for the removal of oil spills and oil/water separation has not yet been reported. Such polymers with a very high surface area (450 ± 15 m^2 g^{-1}) can offer rapid and highly efficient removal of oils and organic solvents. The crude oil, diesel and gasoline sorption performance of the nanofibrous mat was compared with the literature (Table S2†). The sorption capacity of the 6FDA–TrMPD mat was higher than many reported adsorbents, including cellulose[30] and mesoporous silica[31] based aerogels and carbon shoot sponge,[13] while the sorption performance was lower than superhydrophobic graphene-based sponge.[32] The main advantages of the 6FDA–TrMPD nanofibrous sorbent for the

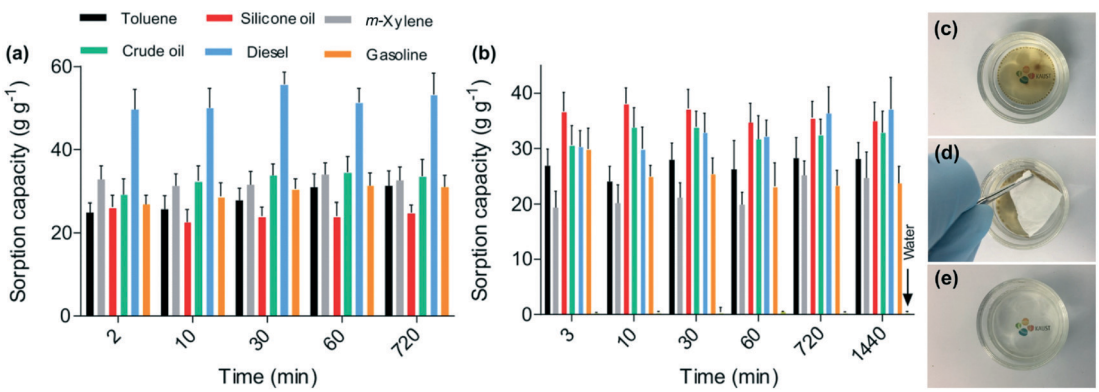

Fig. 6 The oil and solvent removal performance of the nanofibrous mat as a function of time using (a) pure oils and organic solvents, and (b) a mixture of pure oils and organic solvents with water as feed solutions. The mat was used for water adsorption as a control to show its hydrophobic nature. Optical photos for the treatment of crude oil spillage on the seawater with the 6FDA–TrMPD nanofibrous mat (c) before, (d) during, and (e) after treatment of an oil spill.

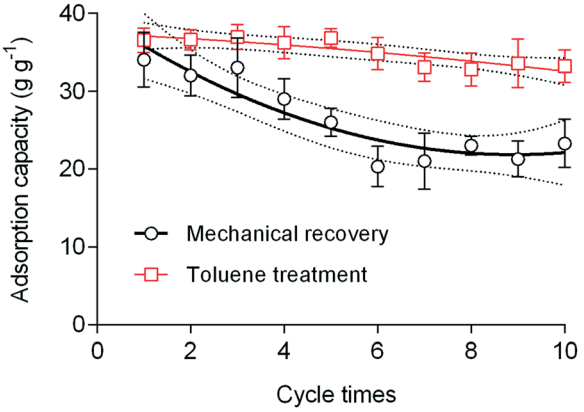

Fig. 7 The reusability of the nanofibrous mat in crude oil removal, employing either mechanical recovery or recovery *via* toluene treatment. Solid and dashed lines denote regressions.

use of oil cleanup are its high intrinsic porosity, therefore rapid removal performance and superoleophilicity, as well as nanofibrous structure with macroporosity for rapid diffusion of oils (Fig. S6†). Furthermore, this highly porous nanofibrous sorbent has also great potential to be employed in water treatment applications for the scavenging of water micropollutants in addition to their use in oil spills cleanup. The monomers are commercially available at affordable prices, and the polymerization is straightforward. Furthermore, our study outlines, for the first time, the use of PIM-based electrospun nanofibers for oil removal. The porous fiber texture described here showed high oil uptake, as verified by the SEM images. Upon contact with oils and organic liquids, the nanofibers instantly adsorb the oils and non-polar liquids, and subsequently released them either by mechanical recovery or treatment with toluene (Fig. 7). Both recovery processes have advantages and disadvantages. We show that the electrospun mat can be reused several times while still maintaining high sorption capacity. SEM analysis of the nanofibers after removal tests clearly shows the swelling of the fibers, rather than interfacial adsorption of oils and organic solvents on the fiber surface.

Conclusions

Hydrophobic nanofibrous electrospun mats from intrinsically microporous polyimide with pendant trifluoromethyl groups were fabricated. The polymer powder was synthesized by a one-step, high-temperature polycondensation reaction, featuring a BET surface area of 450 ± 15 $m^2\ g^{-1}$, which increased to 565 ± 18 $m^2\ g^{-1}$ for the electrospun mat. Ultrafine nanofibers with a mean diameter of 280 nm and by optimizing the different parameters during the electrospinning process, were successfully obtained. The adsorption capacities of the electrospun mats for crude oil, gasoline, diesel, silicone oil, *m*-xylene, and toluene were in the range of 25–56 g g^{-1}. The sorbent showed the highest affinity for diesel with a sorption capacity of 56 g g^{-1}. We attributed the observed high sorption capacities to the uptake of oil and non-polar compounds inside the fiber matrix, thanks to the hierarchically porous nature of the material rather than their adsorption onto the surface, as confirmed by SEM analysis. The robustness of the mats was successfully demonstrated through regeneration cycles using both mechanical pressing and toluene treatment. The mats have the potential to be applied on a large scale for the scavenging of oil and chemical leakages because the mats can be easily upscaled by using industrial electrospinners, reaching maximum sorption capacities up to 56 times their original weights.

Conflicts of interest

There are no conflicts to declare.

Acknowledgements

The authors thank Fadhilah Alduraiei for her technical assistance with some of the electrospinning experiments. The graphical abstract and Fig. 1 were created by Xavier Pita, scientific illustrator at King Abdullah University of Science and Technology (KAUST). The research reported in this publication was supported by funding from KAUST.

Notes and references

1 A. Jernelöv, How to defend against future oil spills, *Nature*, 2010, **466**, 182, DOI: 10.1038/466182a.
2 H. Li and M. C. Boufadel, Long-term persistence of oil from the Exxon Valdez spill in two-layer beaches, *Nat. Geosci.*, 2010, **3**, 96, DOI: 10.1038/ngeo749.
3 P. D. Boehm, D. L. Fiest, D. Mackay and S. Paterson, Physical-chemical weathering of petroleum hydrocarbons from the IXTOC I blowout: chemical measurements and a weathering model, *Environ. Sci. Technol.*, 1982, **16**, 498, DOI: 10.1021/es00102a014.
4 R. C. Prince, J. D. Butler and A. D. Redman, The rate of crude oil biodegradation in the sea, *Environ. Sci. Technol.*, 2017, **51**, 1278, DOI: 10.1021/acs.est.6b03207.
5 P. F. Kingston, Long-term environmental impact of oil spills, *Spill Sci. Technol. Bull.*, 2002, **7**, 53, DOI: 10.1016/S1353-2561(02)00051-8.
6 B. Chen, Q. Ma, C. Tan, T.-T. Lim, L. Huang and H. Zhang, Carbon-based sorbents with three-dimensional architectures for water remediation, *Small*, 2015, **11**, 3319, DOI: 10.1002/smll.201403729.
7 J. Sayyad Amin, M. Vared Abkenar and S. Zendehboudi, Natural sorbent for oil spill cleanup from water surface: environmental implication, *Ind. Eng. Chem. Res.*, 2015, **54**, 10615, DOI: 10.1021/acs.iecr.5b01715.
8 V. Singh, S. Jinka, K. Hake, S. Parameswaran, R. J. Kendall and S. Ramkumar, Novel natural sorbent for oil spill cleanup, *Ind. Eng. Chem. Res.*, 2014, **53**, 11954, DOI: 10.1021/ie5019436.
9 M. M. Radetić, D. M. Jocić, P. M. Jovančić, Z. L. Petrović and H. F. Thomas, Recycled wool-based nonwoven material as an oil sorbent, *Environ. Sci. Technol.*, 2003, **37**, 1008, DOI: 10.1021/es0201303.

10 Z. Wang, P. Jin, M. Wang, G. Wu, C. Dong and A. Wu, Biomass-derived porous carbonaceous aerogel as sorbent for oil-spill remediation, *ACS Appl. Mater. Interfaces*, 2016, **8**, 32862, DOI: 10.1021/acsami.6b11648.

11 H. Zhu, S. Qiu, W. Jiang, D. Wu and C. Zhang, Evaluation of electrospun polyvinyl chloride/polystyrene fibers as sorbent materials for oil spill cleanup, *Environ. Sci. Technol.*, 2011, **45**, 4527, DOI: 10.1021/es2002343.

12 H.-Y. Mi, X. Jing, Y. Liu, L. Li, H. Li, X.-F. Peng and H. Zhou, Highly durable superhydrophobic polymer foams fabricated by extrusion and supercritical CO2 foaming for selective oil absorption, *ACS Appl. Mater. Interfaces*, 2019, **11**, 7479, DOI: 10.1021/acsami.8b21858.

13 Y. Gao, Y. S. Zhou, W. Xiong, M. Wang, L. Fan, H. Rabiee-Golgir, L. Jiang, W. Hou, X. Huang, L. Jiang, J.-F. Silvain and Y. F. Lu, Highly efficient and recyclable carbon soot sponge for oil cleanup, *ACS Appl. Mater. Interfaces*, 2014, **6**, 5924, DOI: 10.1021/am500870f.

14 Y. Chu and Q. Pan, Three-dimensionally macroporous Fe/C nanocomposites as highly selective oil-absorption materials, *ACS Appl. Mater. Interfaces*, 2012, **4**, 2420, DOI: 10.1021/am3000825.

15 J. T. Korhonen, M. Kettunen, R. H. A. Ras and O. Ikkala, Hydrophobic nanocellulose aerogels as floating, sustainable, reusable, and recyclable oil absorbents, *ACS Appl. Mater. Interfaces*, 2011, **3**, 1813, DOI: 10.1021/am200475b.

16 A. Zhang, M. Chen, C. Du, H. Guo, H. Bai and L. Li, Poly(dimethylsiloxane) oil absorbent with a three-dimensionally interconnected porous structure and swellable skeleton, *ACS Appl. Mater. Interfaces*, 2013, **5**, 10201, DOI: 10.1021/am4029203.

17 H. Bi, X. Xie, K. Yin, Y. Zhou, S. Wan, L. He, F. Xu, F. Banhart, L. Sun and R. S. Ruoff, Spongy graphene as a highly efficient and recyclable sorbent for oils and organic solvents, *Adv. Funct. Mater.*, 2012, **22**, 4421, DOI: 10.1002/adfm.201200888.

18 J.-C. Wang, H. Lou, Z.-H. Cui, Y. Hou, Y. Li, Y. Zhang, K. Jiang, W. Shi and L. Qu, Fabrication of porous polyacrylamide/polystyrene fibrous membranes for efficient oil-water separation, *Sep. Purif. Technol.*, 2019, **222**, 278, DOI: 10.1016/j.seppur.2019.04.044.

19 Z. Zhang, Y. Yang, C. Li and R. Liu, Porous nanofibrous superhydrophobic membrane with embedded Au nanoparticles for the integration of oil/water separation and catalytic degradation, *J. Membr. Sci.*, 2019, **582**, 350, DOI: 10.1016/j.memsci.2019.04.024.

20 Z. Shami, A. Gharloghi and S. M. Amininasab, Multifunctional pH-switched superwetting copolymer nanotextile: surface engineered toward on-demand light oil-water separation on superhydrophilic–underwater low-adhesive superoleophobic nonwoven mesh, *ACS Sustainable Chem. Eng.*, 2019, **7**, 8917, DOI: 10.1021/acssuschemeng.9b00931.

21 W. Ma, M. Zhang, Y. Li, M. Kang, C. Huang and G. Fu, Flexible, durable and magnetic nanofibrous membrane with pH-switchable wettability for efficient on-demand oil/water separation, *Environ. Sci.: Nano*, 2019, **6**, 3699, DOI: 10.1039/C9EN01023H.

22 A. Ghaffar, C. Chen, X. Zhu and B. Chen, Underwater superoleophobic PVA–GO nanofibrous membranes for emulsified oily water purification, *Environ. Sci.: Nano*, 2019, **6**, 3723, DOI: 10.1039/C9EN00883G.

23 Z. Li, C. M. Tan, W. Tio, J. Ang and D. D. Sun, Manta ray gill inspired radially distributed nanofibrous membrane for efficient and continuous oil-water separation, *Environ. Sci.: Nano*, 2018, **5**, 1466, DOI: 10.1039/C8EN00258D.

24 C. Zhang, P. Li and B. Cao, Electrospun microfibrous membranes based on PIM-1/POSS with high oil wettability for separation of oil-water mixtures and cleanup of oil Soluble contaminants, *Ind. Eng. Chem. Res.*, 2015, **54**, 8772, DOI: 10.1021/acs.iecr.5b02321.

25 B. Satilmis and T. Uyar, Superhydrophobic hexamethylene diisocyanate modified hydrolyzed polymers of intrinsic microporosity electrospun ultrafine fibrous membrane for the adsorption of organic compounds and oil/water separation, *ACS Appl. Nano Mater.*, 2018, **1**, 1631, DOI: 10.1021/acsanm.8b00115.

26 J. Zhang, F. Zhang, J. Song, L. Liu, Y. Si, J. Yu and B. Ding, Electrospun flexible nanofibrous membranes for oil/water separation, *J. Mater. Chem. A*, 2019, **7**, 20075, DOI: 10.1039/C9TA07296A.

27 M. A. Abdulhamid, G. Genduso, Y. Wang, X. Ma and I. Pinnau, Plasticization-resistant carboxyl-functionalized 6FDA-polyimide of intrinsic microporosity (PIM–PI) for membrane-based gas separation, *Ind. Eng. Chem. Res.*, 2019, DOI: 10.1021/acs.iecr.9b04994.

28 X. Yuan, Y. Zhang, C. Dong and J. Sheng, Morphology of ultrafine polysulfone fibers prepared by electrospinning, *Polym. Int.*, 2004, **53**, 1704, DOI: 10.1002/pi.1538.

29 A. Veerabhadraiah, S. Ramakrishna, G. Angadi, M. Venkatram, V. Kanivebagilu Ananthapadmanabha, N. M. Hebbale NarayanaRao and K. Munishamaiah, Development of polyvinyl acetate thin films by electrospinning for sensor applications, *Appl. Nanosci.*, 2017, **7**, 355, DOI: 10.1007/s13204-017-0576-9.

30 S. T. Nguyen, J. Feng, N. T. Le, A. T. T. Le, N. Hoang, V. B. C. Tan and H. M. Duong, Cellulose Aerogel from Paper Waste for Crude Oil Spill Cleaning, *Ind. Eng. Chem. Res.*, 2013, **52**, 18386–18391, DOI: 10.1021/ie4032567.

31 Q. Shuai, X. Yang, Y. Luo, H. Tang, X. Luo, Y. Tan and M. Ma, A superhydrophobic poly(dimethylsiloxane)-TiO2 coated polyurethane sponge for selective absorption of oil from water, *Mater. Chem. Phys.*, 2015, **162**, 94–99, DOI: 10.1016/j.matchemphys.2015.05.011.

32 R.-F. Shiu, C.-L. Lee, P.-Y. Hsieh, C.-S. Chen, Y.-Y. Kang, W.-C. Chin and N.-H. Tai, Superhydrophobic graphene-based sponge as a novel sorbent for crude oil removal under various environmental conditions, *Chemosphere*, 2018, **207**, 110–117, DOI: 10.1016/j.chemosphere.2018.05.071.

